MOLECULAR AND CELLULAR BIOLOGY, Feb. 2006, p. 965–975 Vol. 26, No. 3
0270-7306/06/$08.00+0 doi:10.1128/MCB.26.3.965–975.2006

Phenotypic Analysis of Mice Lacking the *Tmprss2*-Encoded Protease

Tom S. Kim,[1] Cynthia Heinlein,[1] Robert C. Hackman,[2] and Peter S. Nelson[1]*

Division of Human Biology[1] and Division of Clinical Research,[2] Fred Hutchinson Cancer Research Center, Mailstop D4-100, 1100 Fairview Avenue North, Seattle, Washington 98109-1024

Received 12 September 2005/Returned for modification 21 October 2005/Accepted 4 November 2005

Tmprss2 **encodes an androgen-regulated type II transmembrane serine protease (TTSP) expressed highly in normal prostate epithelium and has been implicated in prostate carcinogenesis. Although in vitro studies suggest protease-activated receptor 2 may be a substrate for TMPRSS2, the in vivo biological activities of TMPRSS2 remain unknown. We generated *Tmprss2*$^{-/-}$ mice by disrupting the serine protease domain through homologous recombination. Compared to wild-type littermates, *Tmprss2*$^{-/-}$ mice developed normally, survived to adulthood with no differences in protein levels of prostatic secretions, and exhibited no discernible abnormalities in organ histology or function. Loss of TMPRSS2 serine protease activity did not influence fertility, reduce survival, result in prostate hyperplasia or carcinoma, or alter prostatic luminal epithelial cell regrowth following castration and androgen replacement. Lack of an observable phenotype in *Tmprss2*$^{-/-}$ mice was not due to transcriptional compensation by closely related *Tmprss2* homologs. We conclude that the lack of a discernible phenotype in *Tmprss2*$^{-/-}$ mice suggests functional redundancy involving one or more of the type II transmembrane serine protease family members or other serine proteases. Alternatively, TMPRSS2 may contribute a specialized but nonvital function that is apparent only in the context of stress, disease, or other systemic perturbation.**

Serine proteases play essential roles in many physiological and pathological processes that include coagulation, digestion, hormone processing, wound healing, embryonic development, immune responses, and cancer progression (reviewed in references 3 and 55). The subfamily of membrane-bound serine proteases represents an important class of these enzymes by virtue of their involvement in cell surface proteolysis with the potential to modulate signal-transducing receptors and other proteins anchored to the cell surface. We have previously shown that *t*rans*m*embrane *pr*otea*s*e, *s*erine *2* (TMPRSS2) is highly expressed in the epithelium of the human prostate gland and is regulated by androgenic hormones (27). TMPRSS2 spans the membrane once near the amino terminus and has a cleavable protease domain in the carboxy terminus, features characteristic of a type II transmembrane serine protease (TTSP) (17).

The human *TMPRSS2* gene comprises 14 exons and is located on chromosome 21q22.2 (21, 35). The murine *Tmprss2* orthologue, also known as epitheliasin, encompasses 14 exons on chromosome 16C4 (20). The human and mouse *Tmprss2* genes encode proteins of 492 and 490 amino acids, respectively, but migrate at a higher molecular mass of ~70 kDa by sodium dodecyl sulfate-polyacrylamide gel electrophoresis (SDS-PAGE) due to glycosylation. In addition to the full-length TMPRSS2 protein, analyses of extracts from tissues and cell lines demonstrate an ~32-kDa polypeptide consistent with the free serine protease domain of TMPRSS2 that results from autoactivated proteolytic cleavage (1). TMPRSS2 is expressed in several human tissues that comprise large populations of epithelial cells (21), with the highest level of transcripts measured in the prostate gland (27). In accord with the human tissue distribution, the mouse prostate and kidney exhibit the highest level of *Tmprss2* expression (20, 21).

The biological functions of mammalian TMPRSS2 have not been determined. TMPRSS2 shares 40.6% amino acid identity and 63% similarity with TMPRSS3, a gene associated with nonsyndromic early childhood deafness (5, 32). Studies with *Xenopus* oocytes have demonstrated that wild-type (WT) TMPRSS3 activates epithelial amiloride-sensitive sodium channels, whereas mutant forms of TMPRSS3, known to cause deafness, fail to activate the sodium channel (15). Other membrane proteases shown to increase sodium channel currents include TMPRSS4 (CAP2) and PRSS14 (CAP3), both of which are TTSPs, and prostasin (CAP1), which is anchored to the plasma membrane by a glycosylphosphatidylinositol linkage (45). In contrast, expression of TMPRSS2 in *Xenopus* oocytes reduced both sodium channel activity and protein levels (12).

Interest in TMPRSS2 function has stemmed from findings of high relative expression levels in the prostate and regulation by androgenic hormones that suggest roles in gland development, contributions to tissue-specific functions, and involvement in pathological processes such as prostate carcinogenesis. Other androgen-regulated proteases expressed by prostate epithelial cells such as prostate-specific antigen, hK2, and KLK4 have been postulated to influence the pathogenesis of prostate neoplasia and have been exploited as biomarkers of cancer development and progression. In this context, TMPRSS2 has been reported to be overexpressed in a cohort of patients with prostate carcinoma (42). One patient with a nonsense mutation expected to inactivate TMPSS2 protease function had an aggressive form of the disease. However, studies designed to determine a correlation between TMPRSS2 germ line polymorphisms and the development of prostate cancer have found no associations (30). In addition to cancer of the prostate, TMPRSS2 is expressed highly in colon carcinomas (1). In vitro experiments have shown that exogenous TMPRSS2 protein is

* Corresponding author. Mailing address: Division of Human Biology, Fred Hutchinson Cancer Research Center, Mailstop D4-100, 1100 Fairview Avenue North, Seattle, WA 98109-1024. Phone: (206) 667-3377. Fax: (206) 667-2917. E-mail: pnelson@fhcrc.org.

able to regulate signaling through protease-activated receptor 2 (PAR2) in the LNCaP prostate cancer cell line (47). PAR1 and PAR2 activation can contribute to tumor cell migration and metastasis (2).

To investigate the biological function of TMPRSS2 in vivo, we generated a mouse strain with the targeted disruption of the *Tmprss2* serine protease domain by homologous recombination in mouse embryonic stem (ES) cells. Mice heterozygous and homozygous for TMPRSS2 protease loss are viable and fertile and exhibit no detectable abnormalities. Specific analyses of prostatic secretions and prostate regeneration following castration identified no discernible differences between wild-type and TMPRSS2 protease-null animals.

MATERIALS AND METHODS

Generation of mice with targeted disruption of the TMPRSS2 protease domain. All animal experiments employed procedures approved by the Fred Hutchinson Cancer Research Center Animal Care Committees and conformed to recommendations of the American Veterinary Medical Association Panel on Euthanasia.

A probe containing nucleotides 90 to 840 of the mouse *Tmprss2* cDNA (NM_015775) was amplified using PCR with primers P1 and P2 (Table 1) and used to isolate a *Tmprss2* genomic clone containing exons 6 to 14 from a 129S4 mouse library (P. Soriano, Fred Hutchinson Cancer Research Center, Seattle, WA). A 4.5-kb 5′ arm was generated by PCR amplification using primers P3 and P4, and a 1.7-kb 3′ arm was amplified using primers P5 and P6. The 5′ arm was subcloned into the NotI and SacII restriction sites of pPGKneolox2 DTA.2 (P. Soriano), whereas the 3′ arm was subcloned into the HindIII and SalI sites. Neomycin (*neo*) was used for positive selection, and diphtheria toxin A fragment was used for negative selection. KOD HiFi polymerase (Novagen, Madison, WI) was used to generate the targeting vector.

Following ligation, the targeting vector was linearized with SacII and electroporated into R1_129 ES cells (33). Colonies were selected in 300 μg/ml G418 for 9 days. Homologous recombination events were screened by Southern blotting and PCR using primers P7 and P8 or P9 and P10 (Fig. 1A), which hybridized to the genomic sequence outside of the targeting arm construct and within the *neo* gene, respectively. Positive clones were microinjected into C57BL6 blastocysts, and the resulting male chimeric mice were screened for germ line transmission. Genotyping by PCR analysis was carried out using primers P11 and P12 for the WT (388 bp) and primers P13 and P14 for targeted deletion (385 bp). The PCR product with primers P7/P8 was cloned and sequenced to verify proper targeting of *Tmprss2*.

qRT-PCR. Total RNA was extracted from the kidneys and prostate gland using the RNeasy kit (QIAGEN, Valencia, CA) according to the manufacturer's protocol. cDNA was synthesized using 1 to 5 μg of total RNA, 0.14 mM oligo(dT) (22-mer) primer, 0.2 mM concentrations of each deoxynucleoside triphosphate, and Superscript II reverse transcriptase (Invitrogen, Carlsbad, CA). Quantitative reverse transcription-PCR (qRT-PCR) was carried out in triplicate for each sample using 20 ng of cDNA, 0.2 μM concentrations of each primer, and SYBR green PCR master mix (Applied Biosystems, San Francisco, CA). To quantitate gene expression, PCR was performed at 95°C for 10 min, followed by 40 cycles of 95°C for 15 s, 60°C for 30 s, and 72°C for 30 s using an ABI Prism 7700 or 7900 sequence detector. Primer specificity was validated by the amplification of a single PCR product, as determined by observing a single dissociation curve and, concordantly, one PCR product on an agarose gel, and no amplification products in the no-template control samples. To control for the amount of template cDNA used, gene expression was normalized to the mouse ribosomal protein *S16* transcript expression.

Relative expression of *Tmprss2* was calculated according to the ABI prism 7700 sequence detection system user bulletin no. 2. Briefly, *Tmprss2* expression was normalized to *S16* and then relative to the expression level at day 7 of embryonic development, using the following formula: $\Delta\Delta CT_{gene(tissue,\ 7\text{-day embryo})} = \Delta CT_{(gene\text{-}s16)\ tissue} - \Delta CT_{(gene\text{-}s16)7\text{-day embryo}}$. Relative expression was $2^{-\Delta\Delta CTgene}$ according to Livak and Schmittgen (29).

Generation of cladogram. Protein sequences were analyzed using ClustalW software program (http://www.ebi.ac.uk/clustalw/) to generate a cladogram phylogenetic tree based around the neighbor-joining method of Saitou and Nei (36).

Analysis of prostate secretions. Seminal vesicle and anterior prostate fluid was released by gentle squeezing and diluted in 500 μl or 200 μl, respectively, of phosphate-buffered saline (PBS) containing protease inhibitors (Complete Mini; Roche, Indianapolis, IN) with or without 1% SDS. Ventral and dorsal lateral prostatic secretions were obtained by scoring the lobes with a 25-gauge needle prior to centrifugation at 20,000 × *g* for 10 min. Protein samples were analyzed on 4 to 12% gradient Bis-Tris gels (Invitrogen, Carlsbad, CA) and stained with Coomassie blue. Protein concentrations were determined by Bradford assay (Bio-Rad, Hercules, CA) using bovine serum albumin as the standard.

Castration and testosterone replacement experiments. Mice at 3 months of age were castrated 2 weeks prior to androgen supplementation with either 12.5 mg continuous release testosterone pellets (Innovative Research, Sarasota, FL) or intraperitoneal injections of dihydroxytestosterone (DHT, 3 μg/g of body weight; Steraloids, Newport, RI) in 90% sesame oil and 10% ethanol daily for 3 days. Bromodeoxyuridine (BrdU) was injected intraperitoneally at 100 μg/g of body weight in PBS 6 h prior to sacrifice the mice.

TABLE 1. Primers used for vector construction, *Tmprss2* transcript analysis, and qRT-PCR

Primer	Sequence (5′–3′)
P1	AAGCCCCATACTGACCTCCTC
P2	GCTCTGGTCTGGTATCCCTT
P3	CCGCGGTTATACCCACCCTTCTCCCTTGA
P4	GCGGCCGCACCACTGGAGGAACCTCAG AATC
P5	AGTGTCGACCACCCCTCTGTTCCCTATCC
P6	AGTAAGCTTACAACCTAACCATCTGGA AGAGG
P7	AATGAGGAAATTGCATCGCATTG
P8	AGAGGACGCATGAGGGAGTTTTC
P9	ATGGCTTCTGAGGCGGAAAGAAC
P10	AATTCTGGCATGGCTTTCCTGGT
P11	ACCTGGAGTATACGGGAACGTGA
P12	GTGAGTGGGTGAAGGTTGGGTAG
P13	TGTGCCCTTGGACAGATGACTC
P14	AGGCCAGAGGCCACTTGTGTAG
P15	CATCCACACACATCCCAAGTCC
P16	CAAAGCAAGACAGCAGCCACAG
P17	TAGCACATTGTCCCAACGGAGA
P18	ACACGGGATACCAGGCTTTCCT
P19	GAACCCAGGCATGATGCTAGA
P20	CACCCCGAAATCCAGCATT
P21	GGCCGCTGGTTACTTTGAAG
P22	TCGTGTCCCCAATCAGCC
P23	TCCTGTGAGGGCTTCAGTGC
P24	CTCCTCTGCCTTTGGCCCTA
P25	ATCACCCCCGAGTGGATTGT
P26	TTCAGGCCCTTGGTTTTCTTG
P27	GATTGAATGCCTCACCAGGAG
P28	CCTTGGTTTTCTTGCAGAAGG
S16F	AGGAGCGATTTGCTGGTGTGGA
S16R	GCTACCAGGGCCTTTGAGATGGA
mmp2F	CTGATAACCTGGATGCCGTCGT
mmp2R	TGCTTCCAAACTTCACGCTCTT
mmp9F	GTCTCGGGAAGGCTCTGCTGTT
mmp9R	CTCTGGGGATCCACCTTCTGAG
par1F	CTGTCTTCCCGCGTCCCTAT
par1R	TAGAAAGAATGAGCGGGGGTTC
par2F	CAGTTTTCCCTCATCCTCGATCA
par2R	GCAGACAGGGGACTATCTGGTG
mTmprss1F	AGCCCCGACTTCTACGGGAAT
mTmprss1R	CATAGCCGCCACCTTGATGTC
mTmprss3F	GATCTCCACCCAATCGTCTCCT
mTmprss3R	TTCGTCAAGCACCAAATCCTGT
mTmprss4F	CACCCCTGCATCTCCCAAAC
mTmprss4R	TGGAAGGGAGAGCCTCCTTGA
mTmprss13F	CCCTGGGCCTTTTCTCTTGG
mTmprss13R	GACCTCCAGCTTGCCTGAGC
mDESC1F	TGGATTGCTTCCAACACTGGTAT
mDESC1R	CCATTTGTGTGTCTCCAAGAACC
mMatriptaseF	GGGGTATAGCAGCATGGACAGAC
mMatriptaseR	GTTCACAGTCTGGGTTGTGTTGG

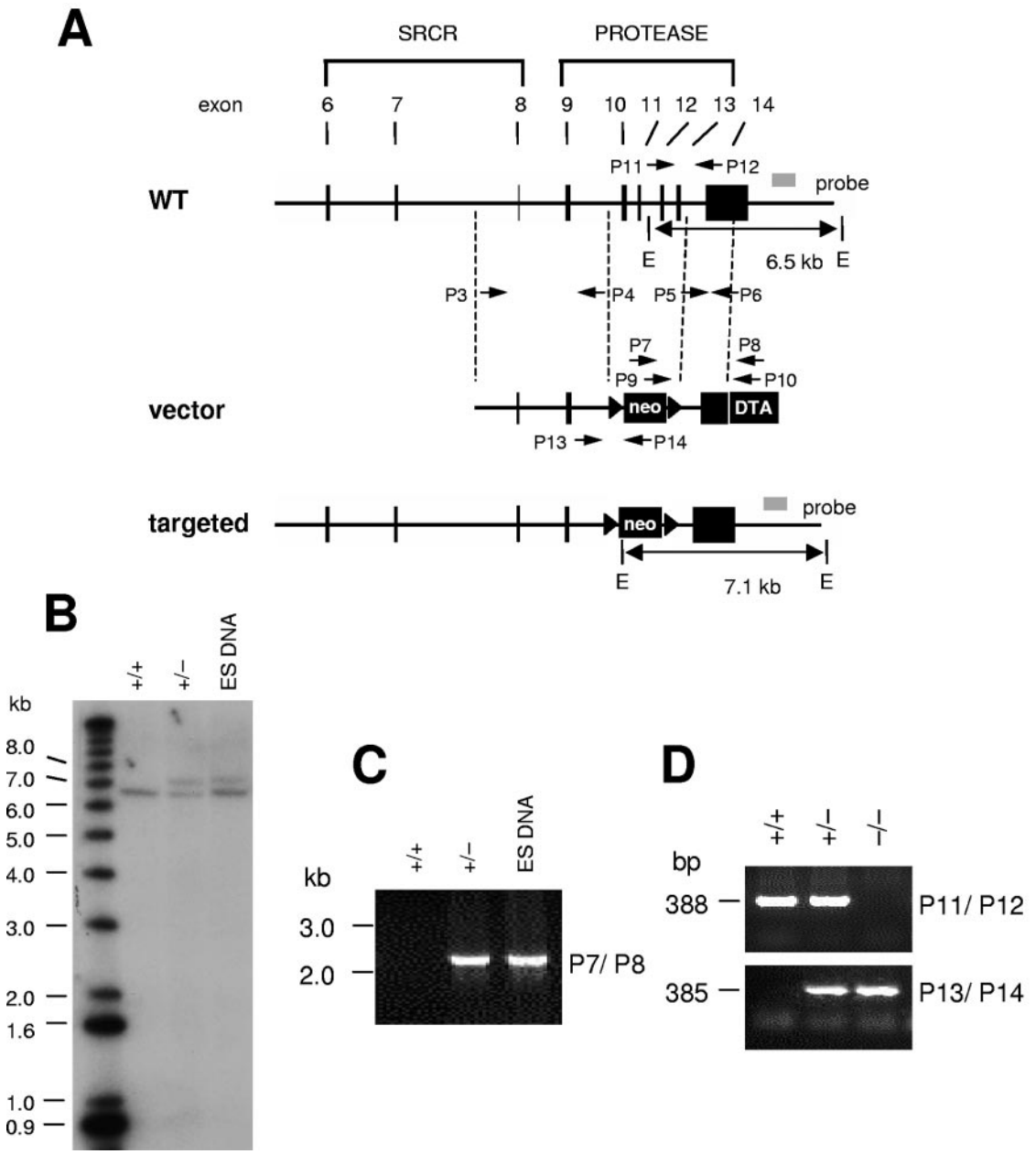

FIG. 1. Generation of the TMPRSS2 protease-null mouse. (A) Schematic diagram of *Tmprss2* genomic organization with exons (black rectangles) 6 to 14, the targeting vector with neomycin (neo) and diphtheria toxin A fragment (DTA) genes, and the targeted allele resulting from a homologous recombination event that replaces exons 10 and 13 with neo. EcoRI (E) restriction enzyme-digested genomic fragments are indicated for the WT (6.5 kb) and targeted (7.1 kb) alleles. The 3′ Southern probe flanking the targeting vector arm is shown as a gray box. Arrows P1 to P14 indicate PCR primers. (B) Southern blot analysis with a 3′ probe (gray). (C) PCR analysis of targeted ES DNA and WT (+/+) or heterozygous (+/−) mouse tail DNA. Primers P7/P8 amplify a 2.25-kb fragment from the targeted allele but not from the WT allele. Additionally, primers P9/P10 amplified a 1.95-kb fragment in the targeted allele but not from the WT allele (data not shown). (D) PCR genotyping of WT (+/+), heterozygous (+/−), and homozygous null (−/−) tail DNA with the indicated primer sets. Primers P11/P12 produce a 388-bp fragment from the WT allele, and primers P13/P14 produce a 385-bp fragment from the targeted allele.

Pathology, histology, and immunohistochemistry. Necropsies were performed on mice aged 2 months to 1 year. Blood samples were collected by cardiac puncture or retro-orbital bleeds. Clinical chemistry, enzymatic assays, and quantitative blood cell measurements were performed by Phoenix Central Laboratories, Everett, WA. Tissues were dissected from the mice, weighed, and immediately fixed in 10% buffered formalin or 4% paraformaldehyde overnight at 4°C. The fixed tissues were washed and stored in 70% ethanol until ready for processing and paraffin embedding. Five-micrometer tissue sections were stained with Harris modified hematoxylin and eosin. For immunohistochemistry, 4-μm sections were deparaffinized in xylene and rehydrated sequentially in 100%, 90%, and 70% ethanol prior to placing the sections in water. The endogenous peroxidase was quenched with 0.3% hydrogen peroxide for 20 min. For Ki 67 staining, antigen was retrieved in 10 mM citrate buffer, pH 6.0, for 20 min in a vegetable steamer followed by blocking in 2% rabbit serum in PBS prior to incubation with anti-Ki 67 antibody (1:500 dilution; Santa Cruz Biotechnology, Santa Cruz, CA). For BrdU staining, DNA was depurinated in 2 N HCl at 37°C for 15 min followed by proteinase K (5 μg/ml) digestion for 15 min

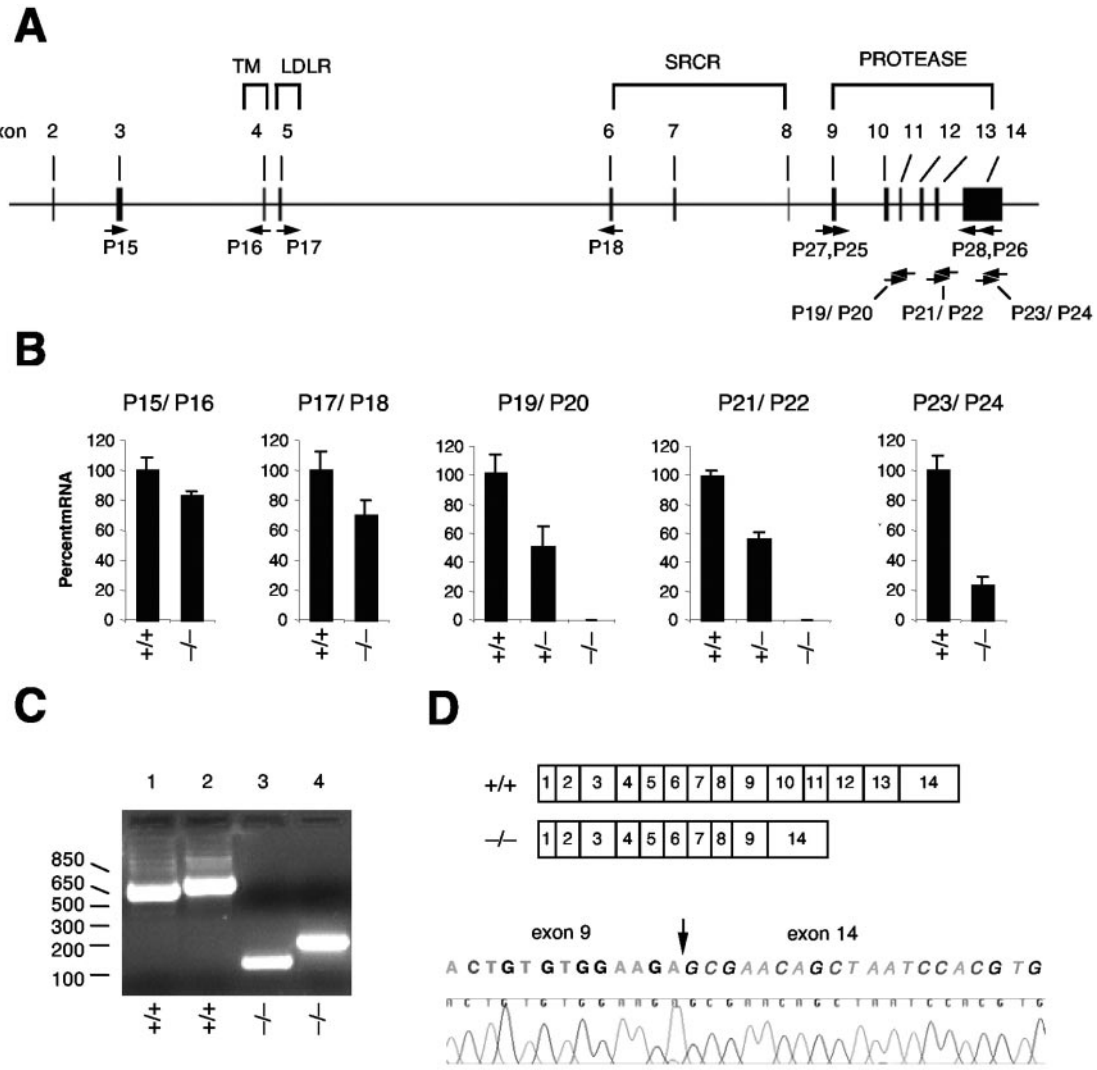

FIG. 2. Expression of *Tmprss2* mRNAs in TMPRSS2 protease-null mice. (A) Primers used for qRT-PCR are shown in context of *Tmprss2* genomic organization. Primers P15/P16 are in exons 3 and 4, respectively, P17/P18 are in exons 5 and 6, respectively, P19/P20 are in exon 11, P21/P22 are in exon 13, P23/P24 are in the 3′ UTR of exon 14, and P25/P26 are in exons 9 and 14, respectively. (B) qRT-PCR analysis of *Tmprss2* mRNA expression using total RNA from kidney of wild-type (+/+), heterozygous (+/−), and homozygous (−/−) mice. The transcript expression level was relative to that in the WT, which was set at 100%. (C) PCR products from wild-type (+/+) and homozygous (−/−) mice using primers P25/P26 and P27/P28, both of which amplify DNA fragments from exon 9 to 14. From the wild-type allele, primers P25/P26 amplified a 671-bp fragment (lane 1), while P27/P28 amplified a 744-bp fragment (lane 2). From the targeted allele, primers P25/P26 amplified a 120-bp fragment (lane 3), while P27/P28 amplified a 196-bp fragment (lane 4). (D) Box diagrams of WT *Tmprss2* and an alternative transcript in the *Tmprss2*$^{-/-}$ mice. The PCR products of P25/P26 and P27/P28 were sequenced to verify that exon 9 is spliced to exon 14; the arrow marks the splice junction.

in 100 mM Tris, pH 8.0, containing 5 mM EDTA. Tissues were blocked in 2% horse serum in PBS prior to incubation with anti-BrdU antibody (1:1,000 dilution; Roche, Indianapolis, IN). After incubation with the appropriate secondary antibody conjugated to biotin, the signal was amplified using the Vectastain elite ABC kit (Vector Labs, Burlingame, CA) and developed using the DAB substrate. Percentages of luminal epithelial cells staining for Ki 67 and BrdU were quantitated by counting 2,000 to 4,000 nuclei, and nuclear staining with an intensity above background was scored as positive.

RESULTS

Generation of mice with targeted disruption of the *Tmprss2* serine protease. To study the physiological function of TMPRSS2, we generated *Tmprss2*$^{-/-}$ mice by deleting exons 10 to 13, which encode 2 of 3 catalytic residues essential for serine protease activity (Fig. 1A). Southern blotting and PCR analysis identified embryonic stem cell clones with the proper homologous recombination event that inserted the neomycin gene into the *Tmprss2* locus. Southern blotting with a 3′ probe outside the targeting vector labeled the predicted EcoRI DNA fragment sizes of 6.5 kb for the WT allele and 7.1 kb for the targeted allele (Fig. 1B). The Southern results were verified by PCR screening using a primer outside the targeting vector arm and another within the *neo* gene (Fig. 1C). Two male chimeras had germ line transmission of the mutant *Tmprss2* allele, clones 1 and 83.

We performed qRT-PCR to determine the expression of *Tmprss2* transcripts in the knockout mice, using primer pairs

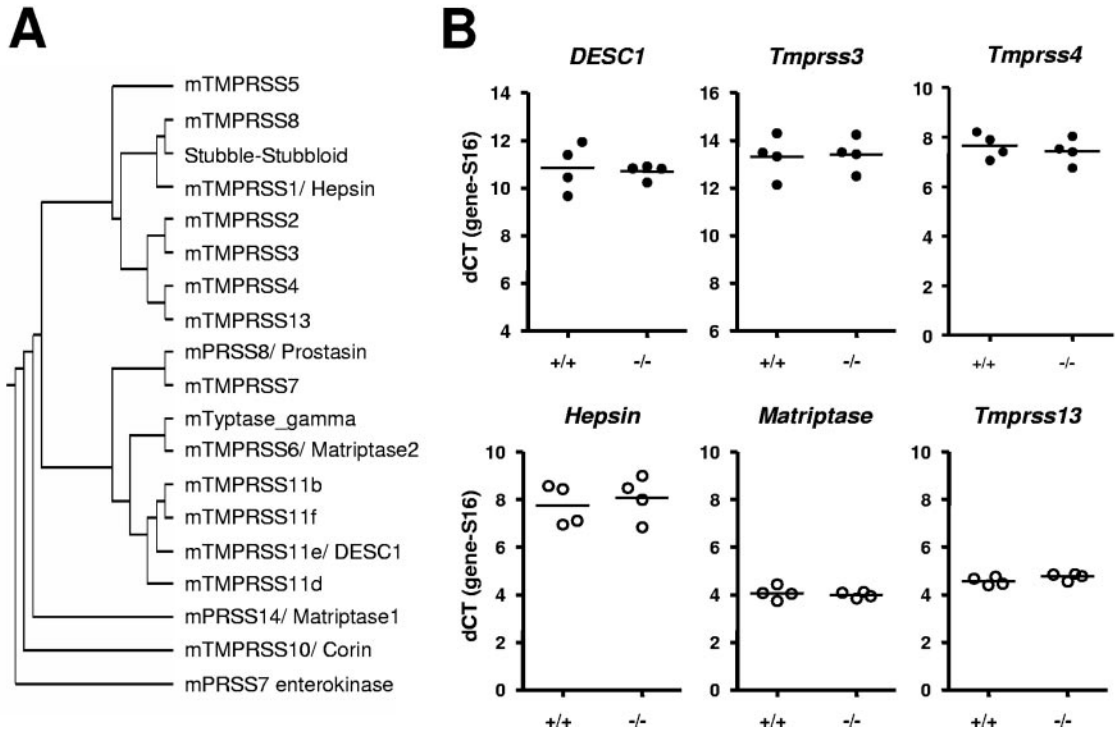

FIG. 3. Expression of TMPRSS2 homologues. (A) Cladogram was generated using the ClustalW program with the protein sequences obtained from the GenBank database as follows: mTMPRSS1/Hepsin, NP_032307.1; mTMPRSS2, NP_056590.2; mTMPSS3, NP_542765.1; mTMPRSS4, NP_663378.1; mTMPRSS5, NP_109634.1; mTMPRSS6, NP_082178.1; mTMPRSS7, AAY66996.1; mTMPRSS8, NP_038949.2; mTMPRSS10, NP_058565.1; mTMPRSS11b, NP_795998.1; mTMPRSS11d, NP_663536.1; mTMPRSS113/DESC1, NP_766468.1; mTMPRSS11f, NP_848845.1; mTMPRSS13, NP_001013391.1; Prss7/Enterokinase, NP_849186.1; mPRSS8/Prostasin, NP_579929.1; Stubble-Stubbloid, NP_476709.1; mPRSS14/Matriptase1, NP_035306.2; mTryptase gamma, NP_036164.1. (B) Gene expression was analyzed by qRT-PCR using 20 ng of cDNA from either the kidney (●) or anterior prostate (○) with primers specific for the indicated protease homologues and normalized to ribosomal protein *S16* mRNA expression. A small difference in cycle threshold (dCT) between the TTSP gene and *S16* indicates higher expression in that tissue.

spanning segments of the cDNA from the 5′ end to the 3′ untranslated region (UTR) (Fig. 2B). qRT-PCR with primers P19/P20 and P21/P22 (Table 1), located in exons 11 and 13, respectively, demonstrated that *Tmprss2*$^{-/-}$ mice do not express this *Tmprss2* transcript. However, only a 20% reduction in *Tmprss2* transcripts was observed in *Tmprss2*$^{-/-}$ mice compared to WT mice when primers spanning exons 3 and 4 (P15/P16) or exons 5 and 6 (P17/P18) were used. Interestingly, when primers in the 3′ UTR (P23/P24) were utilized to quantitate *Tmprss2* gene expression, *Tmprss2*$^{-/-}$ mice had 80% less transcript than WT mice. To ascertain the discrepancy between the transcript measurements, we performed qRT-PCR with primers between exons 9 and 14, which span the exons targeted for disruption. Two different sets of primers (P25/P26 and P27/P28) amplified larger PCR fragments from the WT allele than from the targeted allele (Fig. 2C, compare lanes 1 and 2 to lanes 3 and 4). Sequence analysis of these PCR fragments revealed that *Tmprss2*$^{-/-}$ mice alternatively splice exon 9 to exon 14 (Fig. 2D).

We next measured the transcript levels of several TTSP homologs with the highest amino acid similarity to TMPRSS2 (Fig. 3A) as well as 2 other proteases, DESC1 and Matriptase1, which have overlapping expression with TMPRSS2 in the kidney or prostate, to determine if a compensatory mechanism was operative. *Tmprss3*, *Tmprss4*, and *Desc1* were not expressed in the prostate, but their expression levels were similar in the kidneys of both the *Tmprss2*$^{-/-}$ and WT animals (Fig. 3B). Likewise, no significant difference in the expression of *Matriptase1*, *Hepsin*, and *Tmprss13* was observed in the prostates of *Tmprss2*$^{-/-}$ and WT mice. These results indicate proper targeted deletion of *Tmprss2*$^{-/-}$ and suggest no transcriptionally based compensation for the loss of *Tmprss2* expression (Fig. 3B). Due to the intermouse variability in the expression of these TTSPs, a subtle compensation by a homologue would be difficult to discern from the normal variation.

Fertility and growth of *Tmprss2*$^{-/-}$ mice. Given the high expression of *Tmprss2* in the prostate and other male and female reproductive organs (Fig. 4), we examined whether the loss of *Tmprss2* had an effect on fertility. Breeding heterozygous *Tmprss2*$^{+/-}$ mice produced litters with genotypes indicative of a Mendelian pattern of inheritance. Both male and female *Tmprss2*$^{-/-}$ mice were fertile and produced litter sizes comparable to those of their WT controls (Table 2). Male *Tmprss2*$^{-/-}$ mice sired litters even at 1 year of age. The effect of TMPRSS2 on growth was monitored by external examination and weight gain as the mice matured. No significant difference in weight was measured at weaning or 6 or 12 months of age for either male or female mice (data not shown). Additionally, we measured kidney weights because of the high level of *Tmprss2* expression in this organ. Again, no difference

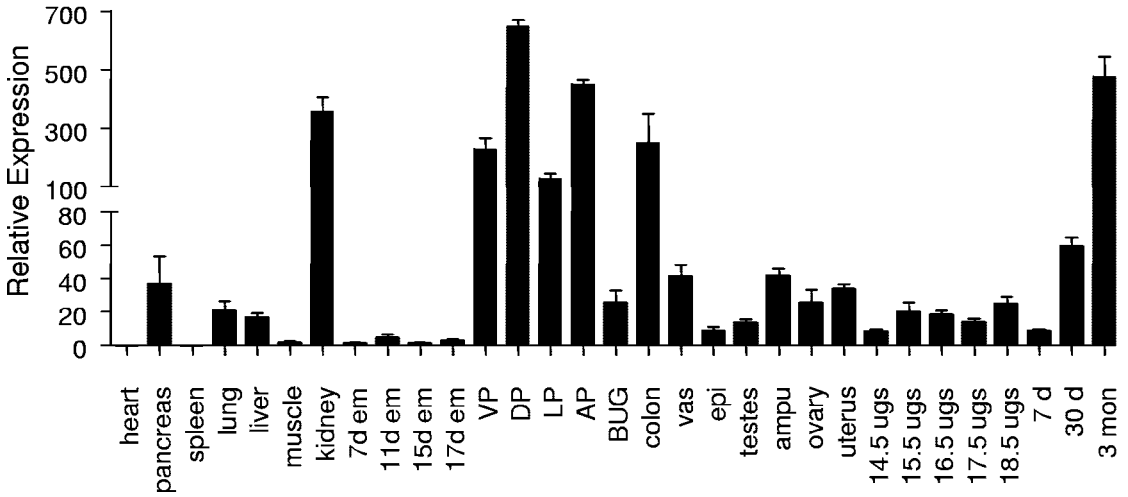

FIG. 4. Tissue distribution of mouse *Tmprss2* transcripts. qRT-PCR was carried out using 20 ng of cDNA from the indicated tissues with primers specific for *Tmprss2* (P21/22) and *s16* genes. *Tmprss2* expression was normalized to *S16* and then presented as expression relative to that observed in a 7-day embryo, which was set to 1. Abbreviations: em, embryo; VP, ventral prostate; DP, dorsal prostate; LP, lateral prostate; AP, anterior prostate; BUG, bulbourethral gland; vas, vas deferens; epi, epididymis; ampu, ampullary gland; ugs, urogenital sinus.

in kidney mass was observed at 1 year of age (data not shown). Both clone 1 and clone 83 *Tmprss2*$^{-/-}$ mice exhibited normal development, survival, and growth up to 14 months of age.

Tissue analysis of *Tmprss2*$^{-/-}$ mice. To determine whether the loss of Tmprss2 had an effect at the microscopic level, we examined the histology of the tissues with the highest levels of *Tmprss2* expression, one of which is the prostate. Androgens are essential for prostate induction, morphogenesis, and differentiation, and the temporal expression of *Tmprss2* mRNA correlates well with testosterone levels, which begin to rise at day 12 of embryogenesis, decrease to baseline levels shortly after birth, and subsequently increase again with age through puberty (Fig. 4) (9). Prostate epithelial buds develop from the urogenital sinus, and the expression of *Tmprss2* in the urogenital sinus (Fig. 4) suggests that it may play a role in prostate induction and morphogenesis. Although *Tmprss2*$^{-/-}$ mice were fertile, we investigated whether the prostate developed normally at the microscopic level. At 2 months of age, the gross anatomy of the *Tmprss2*$^{-/-}$ prostate appeared similar to that of its WT littermate prostate. Microscopically, no discernible differences were observed in the prostate sections of 2-month-old mice stained with hematoxylin and eosin (data not shown). At 1 year of age, all four prostatic lobes of *Tmprss2*$^{-/-}$ and WT mice displayed glands predominantly lined with a single layer of continuous luminal epithelial cells overlying an interspersed discontinuous layer of basal epithelial cells. In addition, sporadic foci of epithelial cell hyperplasia were observed as indicated in Fig. 5A. The number of foci and severity of epithelial hyperplasia were similar in the *Tmprss2*$^{-/-}$ and WT prostates.

Previous immunohistochemical and in situ studies restricted the expression of TMPRSS2 to the distal convoluted tubules, collecting tubules, and papillary epithelium of the kidney and localized it to the apical side of luminal epithelial cells (20, 43). Microscopically, the morphology of the glomeruli, distal and proximal convoluted tubules, and collecting tubules appeared normal in the *Tmprss2*$^{-/-}$ animals (Fig. 5B). Consistent with the kidney weight and histology data, *Tmprss2*$^{-/-}$ kidneys appeared to have normal renal function as determined by the serum biochemical indicators such as creatinine and blood urea nitrogen (Table 3). Additionally, similar levels of total protein and albumin in the plasma demonstrate that kidney function is not compromised in *Tmprss2*$^{-/-}$ mice. The small intestine (43) and colon express *Tmprss2* mRNA at levels similar to that present in the kidney and ventral prostate (Fig. 4). Grossly, at 2 months and 1 year, the stomach and small intestine appeared normal without distension or blockage, and the animals had regular bowel movements, indicating normal digestion, absorption, and peristaltic movement of food. Concordantly, the colon displayed no obvious difference in tissue architecture, and the ordered migration of globet and absorptive cells toward the luminal surface can be observed in Fig. 5B. The pancreas, testes, lung, liver, ovary, and uterus express *Tmprss2* (Fig. 4), and these tissues were also grossly and histologically indistinguishable between *Tmprss2*$^{-/-}$ and WT mice.

Expression of protease-activated receptors in *Tmprss2*$^{-/-}$ mice. The physiological substrate(s) for TMPRSS2 is unknown. Recent in vitro studies suggest that PAR2 is a potential substrate of human TMPRSS2 in cell lines derived from prostate carcinoma (47). Further, treating several different prostate cancer cell lines with a PAR2-activating peptide increased MMP2 and MMP9 enzymatic activity (48), and activation of PAR2 induced *Mmp9* mRNA transcription in a surface airway

TABLE 2. Fertility of *Tmprss2* null mice[a]

Sex (*n*)	Genotype	No. of litters	No. of pups/litter
Male (9)	−/−	17	8.8 ± 1.4
Male (7)	+/+	18	7.7 ± 1.2
Female (10)	−/−	17	8.4 ± 1.8
Female (6)	+/+	13	7.8 ± 1.3

[a] Data are expressed as averages ± standard deviations.

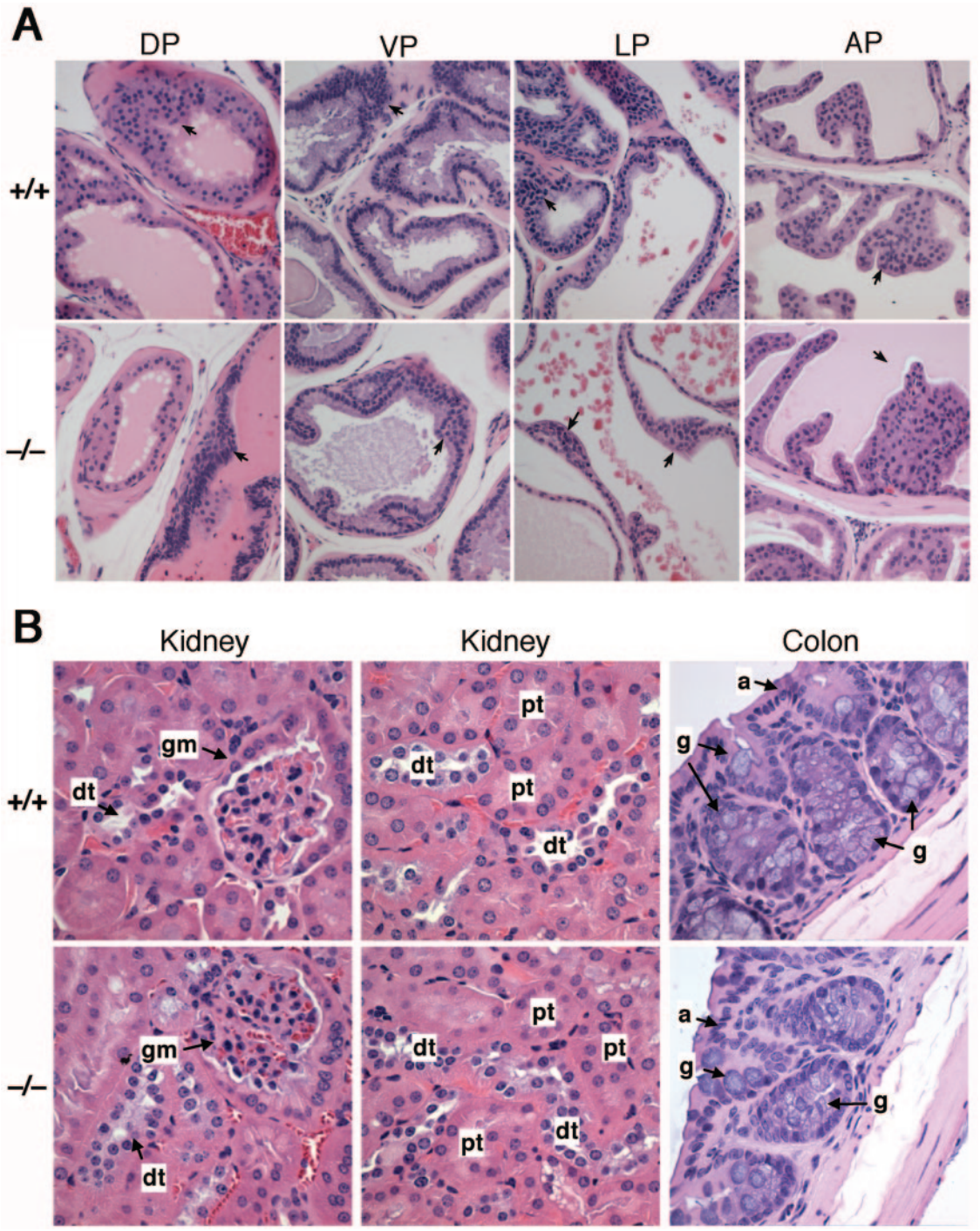

FIG. 5. Histology of selected tissues in *Tmprss2*$^{+/+}$ and *Tmprss2*$^{-/-}$ mice at 1 year of age. (A) Hematoxylin and eosin (H&E)-stained sections of the different prostatic lobes: dorsal (DP), ventral (VP), lateral (LP), and anterior (AP). Magnification, ×200. (B) H&E-stained sections of the kidney cortex and the proximal colon show similar morphology of the glomerulus (gm), distal tubule (dt), proximal tubule (pt), absorptive cells (a), and globlet cells (g) for both genotypes. Magnification, ×400.

epithelial cell line (44). Given these results along with the overlapping expression of PAR1 and PAR2 in the kidney (6, 10) and prostate (48), we examined whether the loss TMPRSS2 protease activity in vivo modulated the transcript levels of *Par1*, *Par2*, *Mmp2*, and *Mmp9*. As shown in Fig. 6, a consistent change in gene expression was not detected in the kidney or anterior prostate by qRT-PCR. However, these genes displayed substantial normal variation with a 2-cycle difference between mice of the same genotype, equal to a fourfold change in mRNA levels, making it difficult to discern if subtle changes in gene expression are due to the targeted deletion of *Tmprss2* or reflect normal variation.

TABLE 3. Clinical chemistry[a]

Analyte	Result for genotype	
	+/+ (n = 3)	−/− (n = 5)
Glucose serum (mg/dl)	152.6 ± 68.7	154.0 ± 57.2
Blood urea nitrogen (mg/dl)	29.6 ± 7.4	24.7 ± 2.1
Creatinine (mg/dl)	0.1 ± 0.1	0.2 ± 0.2
Calcium (mg/dl)	9.6 ± 0.4	9.6 ± 0.7
Phosphorus (mg/dl)	9.1 ± 0.8	8.8 ± 1.6
Total protein (g/dl)	5.8 ± 0.7	5.4 ± 0.5
Albumin (g/dl)	3.4 ± 0.3	3.2 ± 0.2
Globulin (g/dl)	2.4 ± 0.6	2.2 ± 0.3
Albumin/globulin ratio	1.5 ± 0.4	1.5 ± 0.2
Alkaline phosphatase (U/liter)	167.2 ± 69.4	142.0 ± 42.8
Alanine aminotransferase (U/liter)	53.3 ± 35.5	44.7 ± 16.9
Asparate aminotransferase (U/liter)	89.2 ± 30.5	73.0 ± 16.6
Cholesterol (mg/dl)	134.8 ± 13.8	121.7 ± 34.3
Hemolytic index (mg/dl)	53.6 ± 20.2	31.7 ± 12.1
Lipemic index (mg/dl)	7.2 ± 3.7	15.3 ± 21.4

[a] Data are expressed as averages ± standard deviations.

Analysis of prostatic and seminal vesicle protein secretions. Prostatic secretions contribute 15 to 30% of the seminal fluid. Given that TMPRSS2 functions as a protease, we examined whether the loss of TMPRSS2 activity may have altered the levels or sizes of proteins secreted into the lumens of the prostate and seminal vesicle. Mouse seminal vesicle fluid exhibits seven major proteins, seminal vesicle secretion (SVS) I to VII, according to their mobility by SDS-PAGE (8), but no differences were observed in the levels or migratory patterns of these proteins between the WT and *Tmprss2*$^{-/-}$ mice (Fig. 7). Anterior prostate and dorsal lateral prostate secretions remained similar between the WT and *Tmprss2*$^{-/-}$ mice. The ventral prostate displayed the highest variability of secreted proteins when analyzed by SDS-PAGE, but no consistent difference was observed (data not shown).

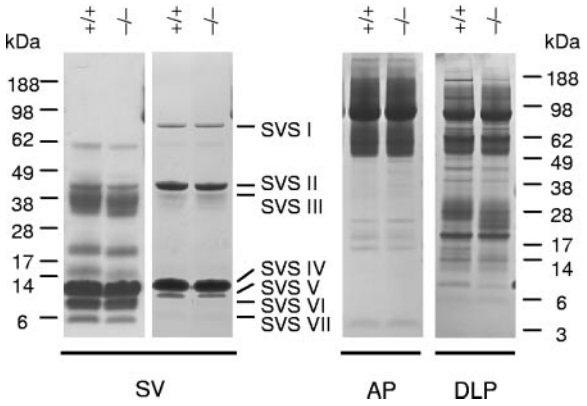

FIG. 7. Analysis of prostatic and seminal vesicle fluid proteins. Protein secretions were extracted from the seminal vesicle (SV) and anterior (AP) and dorsal lateral (DLP) lobes of 3-month-old males and diluted in PBS with or without SDS (all the samples have SDS except lanes 3 and 4). Twenty micrograms of protein was resolved on a 4 to 12% gradient SDS-polyacrylamide gel and stained with Coomassie blue (n = 4 for each genotype).

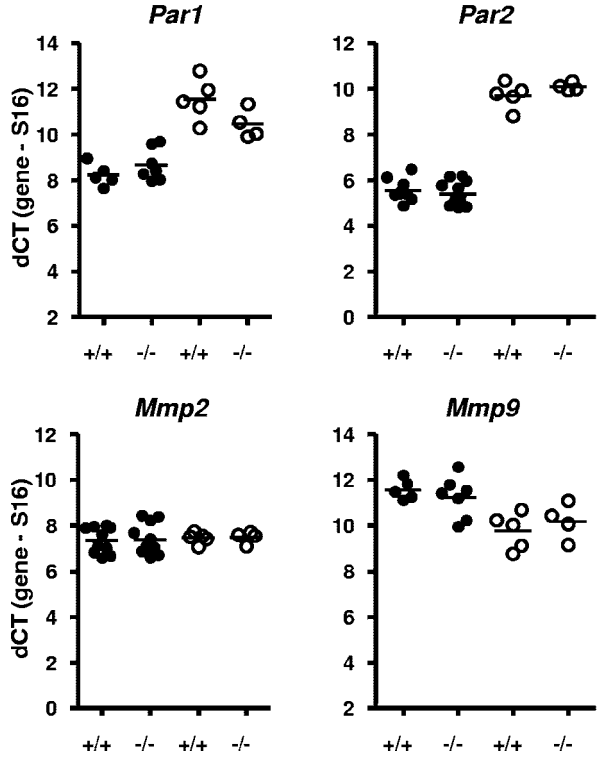

FIG. 6. Expression of *Par1*, *Par2*, *Mmp2*, and *Mmp9* in TMPRSS2 protease-null mice. qRT-PCR was performed using 20 ng of kidney (●) or anterior prostate (○) cDNA with primers specific for the indicated genes. The expression of each gene was normalized to *S16* transcript levels and presented as the difference in cycle threshold (dCT). Each data point represents the average of the results from triplicate qRT-PCR assays for each sample, and the black line represents the mean of each group.

Regeneration of prostate epithelium following castration and testosterone replacement. The prostatic secretory epithelium is dependent upon androgens for survival and function. We examined the role of TMPRSS2 during regeneration of the prostate epithelium using the castration androgen replacement model. At 3 months of age, mice were castrated 2 weeks prior to DHT replacement for 72 h, a time of maximum luminal epithelial cell proliferation (13, 19). No significant difference was observed in the percentage of cells expressing the proliferation marker Ki 67 between the WT and *Tmprss2*$^{-/-}$ mice (Fig. 8). Concordantly, based on BrdU staining, the number of luminal epithelial cells in S phase was similar between WT and *Tmprss2*$^{-/-}$ mice. No differences in the architecture of the prostate glandular structures or stroma were discernible between the *Tmprss2* genotypes either with castration or after androgen supplementation. Thus, loss of the TMPRSS2 protease does not appear to play a role in the survival or proliferation of prostate epithelial cells during castration or prostate regeneration.

DISCUSSION

Loss-of-function alterations in members of the TTSP family has been associated with developmental abnormalities in model organisms. The topology of TTSPs provides an ideal structure for modulating reciprocal cellular interactions with the tissue microenvironment that includes cell proteins localized to the plasma membrane, extracellular matrix components,

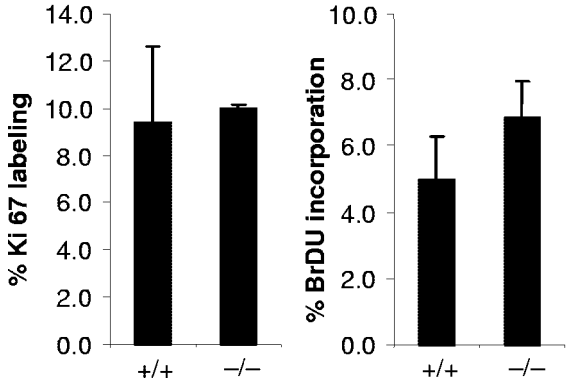

FIG. 8. Prostate regeneration following castration and androgen replacement. Mice at 3 months of age were castrated 2 weeks prior to injection of DHT daily for 3 days and BrdU 6 h before sacrifice. Prostate luminal epithelial cell proliferation in *Tmprss2*$^{-/-}$ mice was assayed by Ki 67 expression or BrdU incorporation using immunohistochemistry. Ki 67 labeling was similar between +/+ mice (9.4% ± 3.2%) and −/− mice (10.0% ± 0.1%), and likewise, BrdU labeling was similar between +/+ mice (5.0% ± 1.3%) and −/− mice (6.9% ± 1.1%). Error bars represent standard deviations (n = 3 to 5 for each genotype).

proteins on neighboring cells, and soluble molecules. Further, the transmembrane and cytoplasmic domains indicate that TTSPs may possibly function as components of signal transduction pathways. For example, the hormonally regulated *Drosophila* TTSP *Stubble* is required for proper leg and wing morphogenesis in the fly. Explanations underlying *Stubble*-mediated influence on organogenesis include protease-mediated regulation of the actin cytoskeleton, cleavage of the extracellular matrix facilitating cell shape changes, activation of cell surface receptors that regulate RhoA signaling, outside-to-inside signal transduction via its cytoplasmic domain, and the mediation of protein-protein interactions through regions other than the protease component of the molecule (4).

To date, the functional roles of three members of the murine TTSP family have been investigated using gene-targeting strategies. Two independent groups disrupted the protease domain of Hepsin, a TTSP expressed predominantly in the liver and at low levels in most other tissues (39). Hepsin has been shown to activate pro-hepatocyte growth factor with the subsequent induction of cMet receptor tyrosine phosphorylation (16, 24), a process known to promote cell growth. Analyses of *Hepsin*$^{-/-}$ mice identified no abnormalities in development, growth, fertility, viability, hemostasis, or liver cell regeneration (49, 50, 53). Corin, a TTSP expressed highly in the heart and at lower levels in testes and kidney (51), has been shown to process pro-atrial natriuretic peptide to its active form in vitro (52). *Corin*$^{-/-}$ mice develop normally, survive to adulthood, and in general, are healthy, with the exception of having hypertension due to decreased levels of active pro-atrial natriuretic peptide (7). In contrast to the relatively minimal effects of *Hepsin* and *Corin* loss, mice with targeted deletions of *St14*/*Matriptase* (*Matriptase*) survived to term but died within 48 h of birth due to dehydration as a result of their grossly aberrant development of the epidermis and hair follicles (28). Matriptase has been shown to activate pro-hepatocyte growth factor, urokinase plasminogen activator, and PAR2 (26, 37). The difference in phenotypes among the TTSP-null mice may reflect the tissue-specific expression patterns, limited primary sequence similarity, and thus, substrate specificity between Matriptase and the other proteases, Hepsin, Corin, and TMPRSS2. However, an intriguing alternative explanation centers on the functional components of the TTSP proteins targeted for disruption in these studies. In addition to the serine protease, transmembrane, and intracellular domains, the TTSP family members contain a stem region that comprise variations of a modular structure consisting of single or repeated sequence motifs that include the group A scavenger receptor domain, low-density lipoprotein receptor class A domain, *C*ls/Clr *u*rchin embryonic growth factor and *b*one morphogenic protein 1 domain, sea urchin sperm protein enterokinase agrin domain, frizzled domain, *m*eprin *A*5 antigen and receptor protein phosphatase μ domain, and a disulfide knotted domain (reviewed in reference 34). The *Matriptase*$^{-/-}$ mice were generated by deleting exon 2, leading to a truncated protein of the N-terminal 27 amino acids whereas *Corin*$^{-/-}$, *Hepsin*$^{-/-}$, and *Tmprss2*$^{-/-}$ mice were generated by targeting the serine protease domain, which in the case of the *Tmprss2*$^{-/-}$ mice reported here, resulted in the expression of a transcript encoding the intracellular, transmembrane, scavenger receptor, and low-density lipoprotein receptor domains. In view of the lack of phenotypic effects observed with loss of protease activities alone, we hypothesize that the stem components may contribute to important unique functions of TTSP members. It will be of interest to specifically disrupt the different domains of the stem region or the protease domain of TTSP members to determine whether these mice have a phenotype similar to that of the mice lacking the entire TTSP protein.

In addition to developmental defects observed with inactivating mutations of *MATRIPTASE* and *TMPRSS3*, the aberrant expression of the several TTSP members has been observed in neoplasms arising in several different organ sites. High levels of *MATRIPTASE* expression in breast carcinoma have been shown to correlate with poor outcome (22). Numerous gene expression profiling studies have identified the near-universal overexpression of *HEPSIN* in primary prostate adenocarcinoma (11, 14, 31). *HEPSIN* is also overexpressed in ovarian cancer (38) and renal cell cancers (18, 54). *TMPRSS3* is overexpressed in ovarian and pancreatic cancer (40), and *TMPRSS4* is overexpressed in pancreatic cancer (46). *CORIN* is expressed in osteosarcoma and endometrial carcinoma cell lines but not in normal uterus cells (51). Studies of TMPRSS2 have demonstrated high levels of expression in colon carcinoma (1) and in prostate cancer cells relative to adjacent benign epithelial cells (42). To determine if Hepsin plays a causative role in the development of prostate cancer, Klezovitch et al. constructed a transgenic mouse with localized expression of Hepsin in prostate epithelium (25). No prostate tumors were observed in these animals, though immunohistochemical studies demonstrated a disruption of the basement membrane surrounding epithelial glands. However, crosses of mice overexpressing Hepsin with the LADY mouse strain engineered to develop localized prostate tumors (23) resulted in the development of metastasis (25). These results suggest that dysregulated proteolysis is an important component of the metastatic process operative in prostate carcinogenesis. It is possible that *Tmprss2* expression could similarly influence the progression of prostate carcinoma, either through protease activity or via signaling events involving other domains of

the protein. In this context, crosses between the *Tmprss2*$^{-/-}$ mice reported here and genetically engineered mouse prostate cancer models could be informative.

In summary, the loss of TMPRSS2 protease did not compromise murine embryonic development, postnatal survival, growth, or normal organ function. Additionally, *Tmprss2*$^{-/-}$ mice appear healthy, exhibit normal behavior, and are fertile even at a year of age. While TMPRSS2 peptides have been identified in human seminal fluid (41), the prostate architecture and secretory protein constituents of the prostate and seminal vesicles were not altered in mice with the loss of this protease. It is possible that TMPRSS2 could exert different effects through different substrate repertoires in the rodent and human reproductive tracts, as the physiological aspects of insemination differ through the liquefaction of seminal fluid in humans and the formation of a copulatory plug in rodents. The lack of a consistent phenotype in *Tmprss2*$^{-/-}$ mice suggests functional redundancy or compensatory mechanisms involving one or more of the type II transmembrane serine protease family members or other serine proteases (34). Generation of multiple-knockout animals could address this possibility. Alternatively, TMPRSS2 may contribute a specialized but not vital function that is apparent only in the context of stress, disease, or other systemic perturbations.

ACKNOWLEDGMENTS

We thank Alice Davy and Josée Aubin for assistance in generating targeting vectors, Carol Ware for ES cell injections, Linda Cherepow for technical expertise in tissue acquisition and processing, Matthew Fero for numerous helpful suggestions and the construction of a mouse breeding database, and Philippe Soriano for 129S4 library and targeting vectors.

T.S.K. was supported by a postdoctoral fellowship from the Canadian Institutes for Health Research. Additional support was provided by NIH grants CA85859 and DK65204 to P.S.N.

REFERENCES

1. **Afar, D. E., I. Vivanco, R. S. Hubert, J. Kuo, E. Chen, D. C. Saffran, A. B. Raitano, and A. Jakobovits.** 2001. Catalytic cleavage of the androgen-regulated TMPRSS2 protease results in its secretion by prostate and prostate cancer epithelia. Cancer Res. **61:**1686–1692.
2. **Bahou, W. F.** 2003. Protease-activated receptors. Curr. Top. Dev. Biol. **54:** 343–369.
3. **Barrett, A. J., N. D. Rawlings, and J. F. Woessner.** 1998. Handbook of proteolytic enzymes, 1st ed. Academic Press, Miami, Fla.
4. **Bayer, C. A., S. R. Halsell, J. W. Fristrom, D. P. Kiehart, and L. von Kalm.** 2003. Genetic interactions between the RhoA and Stubble-stubbloid loci suggest a role for a type II transmembrane serine protease in intracellular signaling during Drosophila imaginal disc morphogenesis. Genetics **165:** 1417–1432.
5. **Ben-Yosef, T., M. Wattenhofer, S. Riazuddin, Z. M. Ahmed, H. S. Scott, J. Kudoh, K. Shibuya, S. E. Antonarakis, B. Bonne-Tamir, U. Radhakrishna, S. Naz, Z. Ahmed, A. Pandya, W. E. Nance, E. R. Wilcox, T. B. Friedman, and R. J. Morell.** 2001. Novel mutations of TMPRSS3 in four DFNB8/B10 families segregating congenital autosomal recessive deafness. J. Med. Genet. **38:**396–400.
6. **Bertog, M., B. Letz, W. Kong, M. Steinhoff, M. A. Higgins, A. Bielfeld-Ackermann, E. Fromter, N. W. Bunnett, and C. Korbmacher.** 1999. Basolateral proteinase-activated receptor (PAR-2) induces chloride secretion in M-1 mouse renal cortical collecting duct cells. J. Physiol. **521**(Pt. 1)**:**3–17.
7. **Chan, J. C., O. Knudson, F. Wu, J. Morser, W. P. Dole, and Q. Wu.** 2005. Hypertension in mice lacking the proatrial natriuretic peptide convertase corin. Proc. Natl. Acad. Sci. USA **102:**785–790.
8. **Chen, Y. H., B. T. Pentecost, J. A. McLachlan, and C. T. Teng.** 1987. The androgen-dependent mouse seminal vesicle secretory protein IV: characterization and complementary deoxyribonucleic acid cloning. Mol. Endocrinol. **1:**707–716.
9. **Corpechot, C., E. E. Baulieu, and P. Robel.** 1981. Testosterone, dihydrotestosterone and androstanediols in plasma, testes and prostates of rats during development. Acta Endocrinol. (Copenhagen). **96:**127–135.
10. **Cunningham, M. A., E. Rondeau, X. Chen, S. R. Coughlin, S. R. Holdsworth, and P. G. Tipping.** 2000. Protease-activated receptor 1 mediates thrombin-dependent, cell-mediated renal inflammation in crescentic glomerulonephritis. J. Exp. Med. **191:**455–462.
11. **Dhanasekaran, S. M., T. R. Barrette, D. Ghosh, R. Shah, S. Varambally, K. Kurachi, K. J. Pienta, M. A. Rubin, and A. M. Chinnaiyan.** 2001. Delineation of prognostic biomarkers in prostate cancer. Nature **412:**822–826.
12. **Donaldson, S. H., A. Hirsh, D. C. Li, G. Holloway, J. Chao, R. C. Boucher, and S. E. Gabriel.** 2002. Regulation of the epithelial sodium channel by serine proteases in human airways. J. Biol. Chem. **277:**8338–8345.
13. **English, H. F., R. J. Santen, and J. T. Isaacs.** 1987. Response of glandular versus basal rat ventral prostatic epithelial cells to androgen withdrawal and replacement. Prostate **11:**229–242.
14. **Ernst, T., M. Hergenhahn, M. Kenzelmann, C. D. Cohen, M. Bonrouhi, A. Weninger, R. Klaren, E. F. Grone, M. Wiesel, C. Gudemann, J. Kuster, W. Schott, G. Staehler, M. Kretzler, M. Hollstein, and H. J. Grone.** 2002. Decrease and gain of gene expression are equally discriminatory markers for prostate carcinoma: a gene expression analysis on total and microdissected prostate tissue. Am. J. Pathol. **160:**2169–2180.
15. **Guipponi, M., G. Vuagniaux, M. Wattenhofer, K. Shibuya, M. Vazquez, L. Dougherty, N. Scamuffa, E. Guida, M. Okui, C. Rossier, M. Hancock, K. Buchet, A. Reymond, E. Hummler, P. L. Marzella, J. Kudoh, N. Shimizu, H. S. Scott, S. E. Antonarakis, and B. C. Rossier.** 2002. The transmembrane serine protease (TMPRSS3) mutated in deafness DFNB8/10 activates the epithelial sodium channel (ENaC) in vitro. Hum. Mol. Genet. **11:**2829–2836.
16. **Herter, S., D. E. Piper, W. Aaron, T. Gabriele, G. Cutler, P. Cao, A. S. Bhatt, Y. Choe, C. S. Craik, N. Walker, D. Meininger, T. Hoey, and R. J. Austin.** 2005. Hepatocyte growth factor is a preferred in vitro substrate for human Hepsin, a membrane-anchored serine protease implicated in prostate and ovarian cancers. Biochem. J. **390:**125–136.
17. **Hooper, J. D., J. A. Clements, J. P. Quigley, and T. M. Antalis.** 2001. Type II transmembrane serine proteases. Insights into an emerging class of cell surface proteolytic enzymes. J. Biol. Chem. **276:**857–860.
18. **Iacobuzio-Donahue, C. A., R. Ashfaq, A. Maitra, N. V. Adsay, G. L. Shen-Ong, K. Berg, M. A. Hollingsworth, J. L. Cameron, C. J. Yeo, S. E. Kern, M. Goggins, and R. H. Hruban.** 2003. Highly expressed genes in pancreatic ductal adenocarcinomas: a comprehensive characterization and comparison of the transcription profiles obtained from three major technologies. Cancer Res. **63:**8614–8622.
19. **Isaacs, J. T.** 1987. Control of cell proliferation and cell death in the normal and neoplastic prostate, p. 85–94. *In* C. H. Rodgers, D. S. Coffey, G. Cunha, J. T. Grayhack, F. Hinman, Jr., and R. Horton (ed.), Benign prostatic hyperplasia, vol. II. National Institutes of Health, Bethesda, Md.
20. **Jacquinet, E., N. V. Rao, G. V. Rao, and J. R. Hoidal.** 2000. Cloning, genomic organization, chromosomal assignment and expression of a novel mosaic serine proteinase: epitheliasin. FEBS Lett. **468:**93–100.
21. **Jacquinet, E., N. V. Rao, G. V. Rao, W. Zhengming, K. H. Albertine, and J. R. Hoidal.** 2001. Cloning and characterization of the cDNA and gene for human epitheliasin. Eur. J. Biochem. **268:**2687–2699.
22. **Kang, J. Y., M. Dolled-Filhart, I. T. Ocal, B. Singh, C. Y. Lin, R. B. Dickson, D. L. Rimm, and R. L. Camp.** 2003. Tissue microarray analysis of hepatocyte growth factor/Met pathway components reveals a role for Met, matriptase, and hepatocyte growth factor activator inhibitor 1 in the progression of node-negative breast cancer. Cancer Res. **63:**1101–1105.
23. **Kasper, S., P. C. Sheppard, Y. Yan, N. Pettigrew, A. D. Borowsky, G. S. Prins, J. G. Dodd, M. L. Duckworth, and R. J. Matusik.** 1998. Development, progression, and androgen-dependence of prostate tumors in probasin-large T antigen transgenic mice: a model for prostate cancer. Lab. Investig. **78:** 319–333.
24. **Kirchhofer, D., M. Peek, M. T. Lipari, K. Billeci, B. Fan, and P. Moran.** 2005. Hepsin activates pro-hepatocyte growth factor and is inhibited by hepatocyte growth factor activator inhibitor-1B (HAI-1B) and HAI-2. FEBS Lett. **579:**1945–1950.
25. **Klezovitch, O., J. Chevillet, J. Mirosevich, R. L. Roberts, R. J. Matusik, and V. Vasioukhin.** 2004. Hepsin promotes prostate cancer progression and metastasis. Cancer Cell **6:**185–195.
26. **Lee, S. L., R. B. Dickson, and C. Y. Lin.** 2000. Activation of hepatocyte growth factor and urokinase/plasminogen activator by matriptase, an epithelial membrane serine protease. J. Biol. Chem. **275:**36720–36725.
27. **Lin, B., C. Ferguson, J. T. White, S. Wang, R. Vessella, L. D. True, L. Hood, and P. S. Nelson.** 1999. Prostate-localized and androgen-regulated expression of the membrane-bound serine protease TMPRSS2. Cancer Res. **59:** 4180–4184.
28. **List, K., C. C. Haudenschild, R. Szabo, W. Chen, S. M. Wahl, W. Swaim, L. H. Engelholm, N. Behrendt, and T. H. Bugge.** 2002. Matriptase/MT-SP1 is required for postnatal survival, epidermal barrier function, hair follicle development, and thymic homeostasis. Oncogene **21:**3765–3779.
29. **Livak, K. J., and T. D. Schmittgen.** 2001. Analysis of relative gene expression data using real-time quantitative PCR and the 2(-Delta Delta C(T)) Method. Methods **25:**402–408.

30. **Lubieniecka, J. M., M. K. Cheteri, J. L. Stanford, and E. A. Ostrander.** 2004. Met160Val polymorphism in the TRMPSS2 gene and risk of prostate cancer in a population-based case-control study. Prostate **59:**357–359.
31. **Magee, J. A., T. Araki, S. Patil, T. Ehrig, L. True, P. A. Humphrey, W. J. Catalona, M. A. Watson, and J. Milbrandt.** 2001. Expression profiling reveals hepsin overexpression in prostate cancer. Cancer Res. **61:**5692–5696.
32. **Masmoudi, S., S. E. Antonarakis, T. Schwede, A. M. Ghorbel, M. Gratri, M. P. Pappasavas, M. Drira, A. Elgaied-Boulila, M. Wattenhofer, C. Rossier, H. S. Scott, H. Ayadi, and M. Guipponi.** 2001. Novel missense mutations of TMPRSS3 in two consanguineous Tunisian families with non-syndromic autosomal recessive deafness. Hum. Mutat. **18:**101–108.
33. **Nagy, A., J. Rossant, R. Nagy, W. Abramow-Newerly, and J. C. Roder.** 1993. Derivation of completely cell culture-derived mice from early-passage embryonic stem cells. Proc. Natl. Acad. Sci. USA **90:**8424–8428.
34. **Netzel-Arnett, S., J. D. Hooper, R. Szabo, E. L. Madison, J. P. Quigley, T. H. Bugge, and T. M. Antalis.** 2003. Membrane anchored serine proteases: a rapidly expanding group of cell surface proteolytic enzymes with potential roles in cancer. Cancer Metastasis Rev. **22:**237–258.
35. **Paoloni-Giacobino, A., H. Chen, M. C. Peitsch, C. Rossier, and S. E. Antonarakis.** 1997. Cloning of the TMPRSS2 gene, which encodes a novel serine protease with transmembrane, LDLRA, and SRCR domains and maps to 21q22.3. Genomics **44:**309–320.
36. **Saitou, N., and M. Nei.** 1987. The neighbor-joining method: a new method for reconstructing phylogenetic trees. Mol. Biol. Evol. **4:**406–425.
37. **Takeuchi, T., J. L. Harris, W. Huang, K. W. Yan, S. R. Coughlin, and C. S. Craik.** 2000. Cellular localization of membrane-type serine protease 1 and identification of protease-activated receptor-2 and single-chain urokinase-type plasminogen activator as substrates. J. Biol. Chem. **275:**26333–26342.
38. **Tanimoto, H., Y. Yan, J. Clarke, S. Korourian, K. Shigemasa, T. H. Parmley, G. P. Parham, and T. J. O'Brien.** 1997. Hepsin, a cell surface serine protease identified in hepatoma cells, is overexpressed in ovarian cancer. Cancer Res. **57:**2884–2887.
39. **Tsuji, A., A. Torres-Rosado, T. Arai, M. M. Le Beau, R. S. Lemons, S. H. Chou, and K. Kurachi.** 1991. Hepsin, a cell membrane-associated protease. Characterization, tissue distribution, and gene localization. J. Biol. Chem. **266:**16948–16953.
40. **Underwood, L. J., K. Shigemasa, H. Tanimoto, J. B. Beard, E. N. Schneider, Y. Wang, T. H. Parmley, and T. J. O'Brien.** 2000. Ovarian tumor cells express a novel multi-domain cell surface serine protease. Biochim. Biophys. Acta **1502:**337–350.
41. **Utleg, A. G., E. C. Yi, T. Xie, P. Shannon, J. T. White, D. R. Goodlett, L. Hood, and B. Lin.** 2003. Proteomic analysis of human prostasomes. Prostate **56:**150–161.
42. **Vaarala, M. H., K. Porvari, A. Kyllonen, O. Lukkarinen, and P. Vihko.** 2001. The TMPRSS2 gene encoding transmembrane serine protease is overexpressed in a majority of prostate cancer patients: detection of mutated TMPRSS2 form in a case of aggressive disease. Int. J. Cancer **94:**705–710.
43. **Vaarala, M. H., K. S. Porvari, S. Kellokumpu, A. P. Kyllonen, and P. T. Vihko.** 2001. Expression of transmembrane serine protease TMPRSS2 in mouse and human tissues. J. Pathol. **193:**134–140.
44. **Vliagoftis, H., A. Schwingshackl, C. D. Milne, M. Duszyk, M. D. Hollenberg, J. L. Wallace, A. D. Befus, and R. Moqbel.** 2000. Proteinase-activated receptor-2-mediated matrix metalloproteinase-9 release from airway epithelial cells. J. Allergy Clin. Immunol. **106:**537–545.
45. **Vuagniaux, G., V. Vallet, N. F. Jaeger, E. Hummler, and B. C. Rossier.** 2002. Synergistic activation of ENaC by three membrane-bound channel-activating serine proteases (mCAP1, mCAP2, and mCAP3) and serum- and glucocorticoid-regulated kinase (Sgk1) in Xenopus oocytes. J. Gen. Physiol. **120:**191–201.
46. **Wallrapp, C., S. Hahnel, F. Muller-Pillasch, B. Burghardt, T. Iwamura, M. Ruthenburger, M. M. Lerch, G. Adler, and T. M. Gress.** 2000. A novel transmembrane serine protease (TMPRSS3) overexpressed in pancreatic cancer. Cancer Res. **60:**2602–2606.
47. **Wilson, S., B. Greer, J. Hooper, A. Zijlstra, J. Quigley, and S. Hawthorne.** 2005. The membrane-anchored serine protease, TMPRSS2, activates PAR-2 in prostate cancer cells. Biochem. J. **388:**967–972.
48. **Wilson, S. R., S. Gallagher, K. Warpeha, and S. J. Hawthorne.** 2004. Amplification of MMP-2 and MMP-9 production by prostate cancer cell lines via activation of protease-activated receptors. Prostate **60:**168–174.
49. **Wu, Q.** 2001. Gene targeting in hemostasis. Hepsin. Front Biosci. **6:**D192–D200.
50. **Wu, Q., D. Yu, J. Post, M. Halks-Miller, J. E. Sadler, and J. Morser.** 1998. Generation and characterization of mice deficient in hepsin, a hepatic transmembrane serine protease. J. Clin. Investig. **101:**321–326.
51. **Yan, W., N. Sheng, M. Seto, J. Morser, and Q. Wu.** 1999. Corin, a mosaic transmembrane serine protease encoded by a novel cDNA from human heart. J. Biol. Chem. **274:**14926–14935.
52. **Yan, W., F. Wu, J. Morser, and Q. Wu.** 2000. Corin, a transmembrane cardiac serine protease, acts as a pro-atrial natriuretic peptide-converting enzyme. Proc. Natl. Acad. Sci. USA **97:**8525–8529.
53. **Yu, I. S., H. J. Chen, Y. S. Lee, P. H. Huang, S. R. Lin, T. W. Tsai, and S. W. Lin.** 2000. Mice deficient in hepsin, a serine protease, exhibit normal embryogenesis and unchanged hepatocyte regeneration ability. Thromb. Haemost. **84:**865–870.
54. **Zacharski, L. R., D. L. Ornstein, V. A. Memoli, S. M. Rousseau, and W. Kisiel.** 1998. Expression of the factor VII activating protease, hepsin, in situ in renal cell carcinoma. Thromb. Haemost. **79:**876–877.
55. **Zucker, S., and W. T. Chen (ed.).** 2003. Cell surface proteases, vol. 54. Academic Press, San Diego, Calif.